
Direct Simultaneous Measurement of Intraglottal Geometry and Velocity Fields in Excised Larynges

Sid Khosla, MD; Liran Oren, PhD; Jun Ying, PhD; Ephraim Gutmark, PhD

Objectives/Hypothesis: Current theories regarding the mechanisms of phonation are based on assumptions about the aerodynamics between the vocal folds during the closing phase of vocal fold vibration. However, many of these fundamental assumptions have never been validated in a tissue model. In this study, the main objective was to determine the aerodynamics (velocity fields) and the geometry of the medial surface of the vocal folds during the closing phase of vibration. The main hypothesis is that intraglottal vortices are produced during vocal fold closing when the glottal duct has a divergent shape and that these vortices are associated with negative pressures.

Study Design: Experiments using seven excised canine larynges.

Methods: The particle imaging velocimetry (PIV) method was used to determine the velocity fields at low, mid-, and high subglottal pressures for each larynx. Modifications were made to previously described PIV methodology to allow the measurement of both the intraglottal velocity fields and the position of the medial aspects of the vocal fold.

Results: At relatively low subglottal pressures, little to no intraglottal vortices were seen. At mid- and high subglottal pressures, the flow separation vortices occurred and produced maximum negative pressures, relative to atmospheric, of -2.6 to -14.6 cm H₂O. Possible physiological and surgical implications are discussed.

Conclusions: Intraglottal vortices produce significant negative pressures at mid- and high subglottal pressures. These vortices may be important in increasing maximum flow declination rate and acoustic intensity.

Key Words: Larynx, phonation, voice, vortices, vocal fold vibration, laryngeal biomechanics, laryngeal aerodynamics, intraglottal geometry, intraglottal velocity fields.

Level of Evidence: N/A.

INTRODUCTION

During phonation, vocal fold vibration converts a steady stream of air supplied by the lungs into a pulsating stream of airflow. When the folds are close enough, airflow through the folds will produce vibration. Vocal fold vibration is an example of “flow-induced oscillations,” a general phenomenon described in engineering literature.¹ The amount of airflow that exits the glottis (superior aspect of the folds) is known as the volumetric flow rate (Q) and is described in terms of the volume of air exiting the vocal folds per a given unit of time, with units such as cm³/sec. Q is constantly changing during

the opening and closing phases of vibration, and this change of volumetric flow rate produces the source of acoustic energy,²⁻⁴ which is then filtered by vocal tract resonance according to classical source-filter theory.⁵ Thus, vocal fold vibration is essential for the production of voiced sounds. However, the specific physiological mechanisms underlying vibration are not completely understood. This study attempts to establish a deeper understanding of the phonatory process through a refinement of procedures, yielding valid results and new interpretations. Essential concepts from voice science and laryngeal biomechanics will also be explained as necessary.

In “Myoelastic-aerodynamic theory of phonation,” Van den Berg⁶ postulated that vocal fold vibration was due to the interaction between vocal fold elasticity and laryngeal aerodynamics. Since Van den Berg’s classical work, significant empirical advances have been made to describe the mucosal wave and show how the glottal geometry changes during vibration.^{7,8} For example, it is known that a coronal section of the membranous vocal fold takes on a convergent shape (the superior glottis is more narrow than the inferior) during vocal fold opening and takes on a divergent shape (the superior glottis is wider than the inferior) during vocal fold closing. Many researchers have also measured the elasticity and other mechanical properties of the vocal fold.^{9,10} Such advances

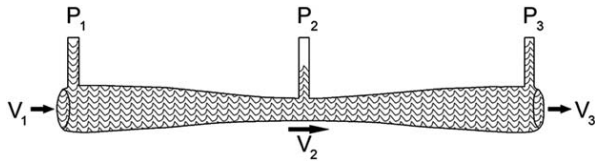


Fig. 1. Flow in a pipe going from left to right. The height of the fluid column is proportional to the pressure. The pipe is convergent from points 1 to 2 (decreasing area) and divergent from points 2 to 3 (increasing area). P = pressure; V = velocity.

in experimental measurements of intraglottal geometry and material characteristics have allowed advances in analytical and computational models of vocal fold dynamics during phonation.^{11–13} In terms of understanding the underlying mechanisms of vibration, experimental measurements are essential for validation of both the results and assumptions of theoretical models, frequently leading to more refined and accurate models. Clinically, accurate models provide specific physiological mechanisms of voice production that could not be obtained by experimentation alone. Models can also be used to understand the pathophysiological mechanisms involved in voice disorders and to predict the effects of different interventions.

For models to be effective, information about the vocal fold material properties and intraglottal geometry is not sufficient. Airflow through the glottis produces intraglottal pressures and forces that will change the shape and separation of the vocal folds and therefore the geometry and diameter of the glottis. The change in the glottal shape then leads to changes in airflow and pressures, which will again result in changes of glottal shape. The resulting vibrations are an example of a general phenomenon known as flow-structure interaction.¹⁴ Thus, understanding both the material properties of the vocal folds and the intraglottal aerodynamics is of vital importance.

However, unlike material properties of the vocal folds, detailed measurements of intraglottal airflow have not been made in tissue models. Instead, researchers have used different theoretical models to study these types of aerodynamics.^{3,11,12,15–17} One problem with these approaches is that they all require basic assumptions regarding intraglottal air velocities and pressures. In order to prove, disprove, or refine current theories, experimental validation is required for both the assumptions and results of a specific theory. In order to provide accurate validation of aerodynamic theories, the most useful experimental data are measurements of intraglottal geometry and intraglottal velocity fields during the closing phase of vibration. The term “field” is used because velocity is a vector that has both a magnitude and direction; both components may vary as a function of spatial location between the folds. The measurement of both the magnitude and direction of the airflow velocity is required because both values can affect the pressure and forces produced by intraglottal airflow.¹⁸

As mentioned previously, the glottis is convergent during opening and divergent during closing. An analogous situation is shown in Figure 1. From point 1 to point 2, the area of the pipe decreases. Similarly during opening, the width and area are smaller at the superior aspect of

the glottis relative to the inferior. The area increases from point 2 to point 3, similar to the shape of the glottis during closing, where the superior aspect of the glottis is wider than the inferior. The reduction and increase in areas are examples of convergence and divergence, respectively. According to the conservation of mass law, if the flow of fluid, such as air, is steady in an enclosed structure such as a pipe, the mass of fluid entering the pipe is equal to the mass exiting—a mathematically equivalent way of stating this is that the volumetric flow rate (Q) will be constant at any location in the pipe.¹⁸ Q is equal to the area of the pipe multiplied by the velocity of the flow. Thus, when a fluid travels from points 1 to 2 in Figure 1, the area decreases and the velocity increases.

Application of this law to the glottis predicts that the velocity will be highest at the most narrow section of the glottis. During closing, the narrowest section is at the inferior aspect of the glottis. During opening, the narrowest section is at the superior edge of the folds. The corresponding pressure distribution can be predicted using Bernoulli’s law, which states that the pressure is inversely proportional to the velocity of the flow. The change of the pressure in the flow is illustrated in Figure 1 by the height of the fluid in the vertical tubes. Thus, when the glottis is divergent, the pressures will be lowest at the inferior aspect of the glottis and highest at the superior aspect. This increase in pressure is known as an adverse pressure gradient (APG). When there is an APG, Bernoulli’s law may not be valid for reasons that have to do with a phenomenon known as *flow separation*.

Flow separation describes a well-known phenomenon in fluid mechanics in which flow separates from an adjacent wall.¹⁸ During the opening phase of vocal fold vibration, the glottis takes on the shape of a converging nozzle and the airflow is attached to the entire medial surface of the vocal folds. In this case, the flow separates from the superior surface of the vocal folds at the glottal exit (see Fig. 2). This assumption is in agreement with the general engineering knowledge of flow in a convergent duct, and there is no controversy about its validity. However, theoretical models do vary in their assumptions about flow separation when the glottis is divergent, which is the typical configuration during the closing phase of vibration. These assumptions can be broadly classified into the following three categories:

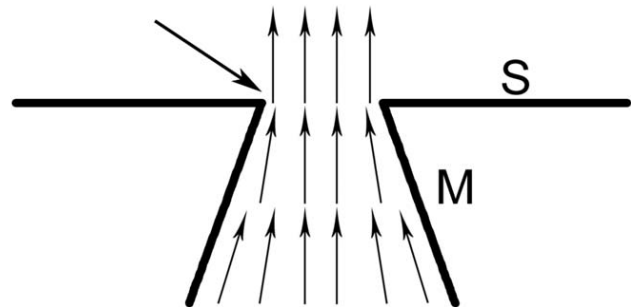


Fig. 2. Convergent cross section of the glottis during opening shows superior surface of fold (S), medial surface (M), and point of flow separation (arrowhead) at the superior aspect of the fold.

Intraglottal Velocity Assumption 1: Flow Separation at the Glottal Exit

These theoretical models^{3,11} assume that flow separation occurs at the glottal exit and not in the glottis for both opening and closing, regardless of glottal shape. This assumption implies that the velocity fields in the glottis will look similar to those represented in Figure 3a. At the superior edge of the folds, the flow does not follow the superior surface of the folds. Thus, the medial-superior aspect of the folds is the location of flow separation because the flow “separates” from all but the most medial aspect of the superior edge of the vocal fold.

Assumption 1 predicts less positive (or even negative) gage pressures in the inferior aspect of the glottis, where the gage pressure is defined as the pressure relative to atmospheric. Positive intraglottal gage pressures produce forces that move the folds laterally, whereas negative intraglottal gage pressures produce forces that move the folds medially. In the myoelastic-aerodynamic theory, Van den Berg⁶ postulated that the “Bernoulli effect” would produce negative pressures relative to atmospheric pressure inside the glottis during the closing phase, causing a suction force. Since then, other theories show that the Bernoulli effect alone does not produce negative or suction pressures, but rather that the combination of Bernoulli’s law and other forces may produce average intraglottal pressures that are less positive (or actually negative) during closing than during opening.^{3,11}

Intraglottal Velocity Field Assumption 2: Recognizes the Existence of Intraglottal Flow Separation With the Assumption That the Resulting Flow Separation Vortices Do Not Produce Any Changes in the Pressure

It is well known in fluid mechanics that, as the diverging angle of the duct exceeds a certain value, the flow cannot follow the duct walls and will separate.¹⁹ This mechanism can produce flow separation from the medial surface *inside* the glottis. The result of this intraglottal flow separation during closing can be the production of rotational airflow or vortices in the glottis. An example of this rotational motion is illustrated in Figure 3b, which can lead to fully formed vortices. These intraglottal vortices will be defined as flow separation vortices (FSV). The mechanism for the formation of the vortices in a divergent duct is well described in the literature¹⁹ and is briefly explained in the discussion. The two key factors for producing FSV are an APG and the viscous interaction between the airflow and the medial surface of the fold. Bernoulli’s law does not account for the effects of viscosity, so it cannot be used to describe or predict the velocity fields associated with these intraglottal vortices. Another limitation of Bernoulli’s law is that it has to be applied along a streamline. Streamlines are lines tangent to the velocity vectors at specified points. In the case of Figure 3a, the streamlines follow the shape of the medial surface of the folds; thus, the usual application of Bernoulli’s law is valid. In Figure 3b, there are two sets of streamlines downstream (toward

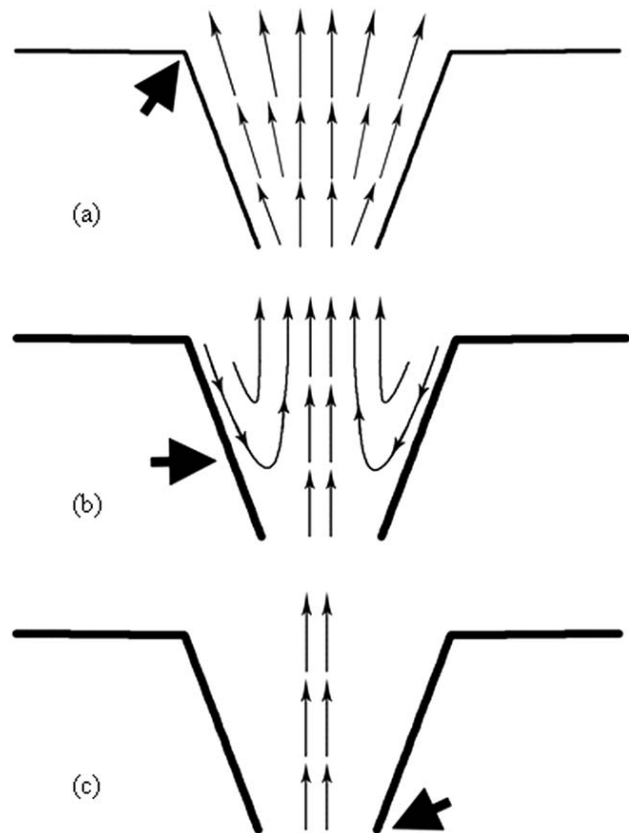


Fig. 3. Three assumptions about flow separation in divergent glottis during closing. The location of the flow separation point is shown by the arrowhead. (a) Separation at superior medial edge. (b) Separation in the middle-to-lower aspect of the glottis. The main straight jet is shown in the middle and the rotation of the separated flow is shown on the sides of the main jet. (c) Flow separation at the inferior aspect of the glottis. The rotational motion shown in (b) is assumed to have minimal velocity and thus is removed. The only remaining flow is the straight jet in the middle.

the superior edge of the folds) of the point of flow separation, which complicates how Bernoulli’s law can be legitimately used.

It is well known in fluid mechanics that vortices are associated with negative gage pressures. Although it is possible to estimate the location of flow separation analytically, determining the negative pressures associated with the intraglottal vortices requires extremely complex computational methods.¹⁷ In order to limit the complexity of their models, investigators have made the approximation that the magnitude of the velocities in the vortices and the associated negative pressures are negligible compared to the main jet.^{12,15,20} Thus, the streamlines associated with the vortices can be removed, resulting in intraglottal velocity fields such as those shown in Figure 3c in which the streamlines of the remaining jet are straight. Different investigators determine the location of flow separation in various ways, but a common assumption for many theoretical models is that the location of separation is the inferior border of the glottis¹²; this location is shown in Figure 3c. There

is a constant distance between the streamlines at the superior edge of the folds compared to the inferior edge. Since Bernoulli's law is taken along the streamlines, the variable that determines area is the distance between the streamlines, not the distance between the folds. A constant distance between the streamlines produces a constant area and, by the conservation of mass law, the velocity will not change. Additionally, models that make this assumption about velocity fields often are based on an assumption that the pressure at the glottal exit is atmospheric (or zero gage pressure). Thus, application of Bernoulli's law along the streamlines results in a prediction of zero gage pressure downstream (toward the superior edge) of the separation point. This assumption leads to the surprising result that airflow through the divergent folds produces a gage pressure of zero between the folds.

Another force that can cause closing is best explained by conceptualizing the elastic, or spring-like, properties of the fold. The spring elements of the fold are compressed during opening and will "spring" back during closing, causing an elastic recoil force (ERF). As long as the compression is relatively small, the magnitude of the ERF is linearly proportional to the amount of compression. If assumption 2 is valid, these recoil forces are the predominant closing force.¹³

Intraglottal Velocity Field Assumption 3: Intraglottal Flow Separation Occurs and Accounts for Significant Negative Gage Pressures Produced by the Flow Separation Vortices

This assumption hypothesizes that the FSV form in the superior aspect of the glottis and produce negative pressures that have a larger magnitude in the superior aspect of the glottis (downstream) as opposed to the inferior aspect (upstream). Unlike assumption 1, the predicted gage pressure is always negative, not merely less positive.

In summary, the three described assumptions predict different vertical pressure distributions in the divergent glottis observed during the closing phase of vibration. Assumption 1 predicts more positive pressures in the superior aspect of the glottis. Assumption 2 predicts that the gage pressure will be zero downstream of the flow separation point. Assumption 3 predicts significant negative pressures in the superior aspect of the glottis, greater in magnitude than the pressures in the inferior aspect. One hypothesis in this article is that assumption 3 is true and that the negative pressures in the superior glottis produce a closing force in addition to the elastic recoil forces. Increased closing forces will result in increased vocal fold closing speed, which has important acoustic consequences that will be discussed later. A schematic of this hypothesis is displayed in Figure 4, which shows fully formed flow separation vortices.

Although there are many analytical, mechanical, and computational models that provide demonstrated or predicted examples intraglottal flow separation,^{16,17,21-24} determining the velocity fields and pressures produced by the vortices is complex and requires computational analy-

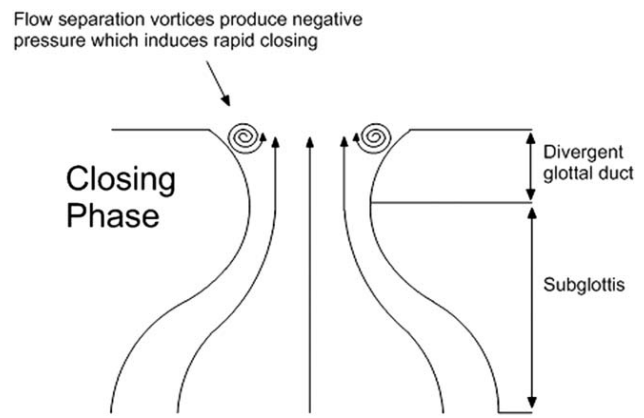


Fig. 4. Intraglottal vortices shown in divergent glottal duct.

sis, specifically techniques using computational flow dynamics (CFD). CFD models must be differentiated in terms of the methodology used. Many CFD models use a technique known as Reynold's Averaging Navier Stokes (RANS); however, more complex, time-intensive, computational algorithms are often necessary to accurately determine pressures generated by vortices. Mihaescu et al.²⁵ showed that Large Eddy Simulation (LES) techniques greatly increased the accuracy of predictions of the velocity fields and pressures when flow separation was present compared to the RANS methodology. Using the LES methodology to model flow in the vocal folds during closing, computational models showed that negative pressures generated by the vortices on the medial surface of the superior half of the vocal fold had a higher magnitude (but opposite sign) than both the pressures on the inferior aspect of the vocal fold and in the subglottal airway.¹⁷ These findings are consistent with assumption 3.

In an excised hemilarynx model, Alipour and Scherer²⁶ showed significant negative pressures during closing that were more negative in the superior aspect of the glottis than in the inferior aspect. These findings also support assumption 3, which states that the FSV produce negative pressures. Although it will not be discussed here, inertance of the air column exiting the glottis has been proposed as a mechanism for producing less positive or even negative pressures in the glottis.³ However, this inertance is only significant if there is a vocal tract. In the experiments conducted by Alipour and Scherer,²⁶ as well as the experiments done in this work, there was no vocal tract present.

In this study, intraglottal velocity fields are measured and the corresponding pressure distributions are calculated. A number of techniques have been used to measure airflow velocity in the larynx. Investigators have used one-dimensional hot-wire anemometry to measure the magnitude of velocities above the vocal folds.^{27,28} However, this technique could not be used to measure intraglottal velocity fields for two reasons. First, in order to avoid damaging the hot wire, the probes must be placed at least one centimeter (cm) above the superior aspect of the folds. However, it has been shown that the velocity fields at the glottal exit are

significantly different from the fields 1 centimeter above the folds.^{29,30} The second limitation is that using a one-dimensional hot-wire probe assumes that airflow travels in only one direction, making quantification of rotational motion and vortical structures impossible. Both the direction and magnitude of the velocity vectors are required to computationally determine the resulting pressure distribution.

Using a technique known as particle imaging velocimetry (PIV), Khosla et al.^{29,30} measured the velocity fields and vortices directly above the glottal exit. In the PIV method, micron-size particles or droplets are injected into the flow in order to render it visible when illuminated. A laser beam spread into a light sheet using a cylindrical lens produces the illumination. The laser is pulsed such that two sheets are produced microseconds apart. Both images of the illuminated flow field are recorded using a specialized camera. Computer analysis of the resulting images correlates the particles in the two images, allowing a displacement field to be calculated. Since the time between the two images is known, a velocity field can be calculated. The advantage of the PIV technique is that it is noninvasive and can give the spatial distribution (magnitude and direction of velocity vectors) in any plane of a complex flow field at a given instance of time. Khosla et al.²⁹ showed that vortices directly above the glottal exit during the mid-to-later part of the closing phase. Using the velocity measurements, they calculated the associated pressures and showed that the vortices produced significant negative pressures. In the published PIV measurements in excised larynges, a major assumption is that the vortices seen directly above the glottal exit during the vocal fold closing phase are due to the FSV formed in the glottis. From a fluid mechanics point of view, this is a reasonable assumption requiring further experimental validation. In addition, the pressures associated with the vortices above the vocal folds may be different from the pressures generated by the intraglottal FSV. In our current investigations, we are interested in the forces on the medial aspect of the folds generated by vocal fold elasticity and intraglottal aerodynamics. Therefore, measurement of intraglottal velocity is absolutely necessary.

In this article, we use a major modification of previous PIV techniques to simultaneously measure intraglottal velocity fields, vocal fold vibrations, and the medial aspect of the folds in a coronal section. From these measurements, the intraglottal pressures during closing can be calculated. In order to determine the importance of the intraglottal FSV, three characteristics must be verified: 1) FSV exist in the superior aspect of the divergent folds during closing. 2) The FSV produce negative pressures. 3) The FSV play an important role in normal vocal fold vibration and voice production. The goal of the studies described in this article is to accomplish the first two described verifications. Future articles will focus on the third.

MATERIALS AND METHODS

This study was performed in accordance with the PHS Policy on Humane Care and Use of Laboratory Animals, the

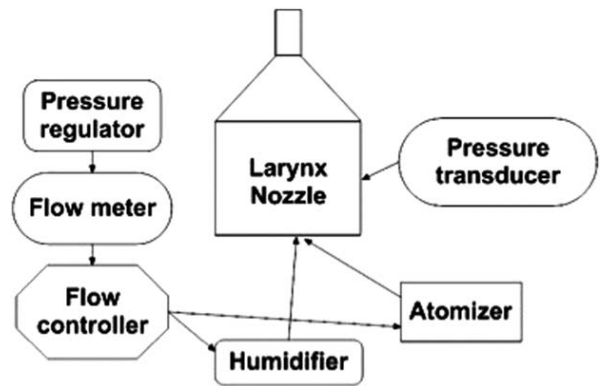


Fig. 5. Schematic of experimental setup.

NIH Guide for the Care and Use of Laboratory Animals, and the Animal Welfare Act (7 U.S.C. et seq.). The animal use protocol was approved by the Institutional Animal Care and Use Committee of the University of Cincinnati School of Medicine. Seven excised larynges were harvested from shared research mongrel canines immediately after the animals were euthanized. All cartilage and soft tissue above the vocal folds were removed, producing an unobstructed view of the vocal folds. A suture was used to adduct the vocal processes and was tied with the minimal tension needed to have a prephonatory width of 0 mm between the vocal processes. Special care was taken to position the suture symmetrically in both the anterior-posterior and inferior-superior directions. The posterior gap, much larger in canine larynges than in humans, was also closed with stitches. The sex and weight of the canine and the length of the membranous folds were, respectively: larynx 1, female, 19 kg, 14.5 mm; larynx 2, female, 17.2 kg, 14.0 mm; larynx 3, male, 17.1 kg, 12.5 mm; larynx 4, female, 19.5 kg, 14.35 mm; larynx 5, male, 15.9 kg, 14.0 mm; larynx 6, male, 15.0 kg, 13.5 mm; and larynx 7, female, 17.2 kg, and 14.0 mm.

The larynges were held in space using four prongs attached to the cricoid. An anterior stitch is placed around the inferior midline of the thyroid cartilage to simulate the cricothyroid muscle and to lengthen the fold. For each larynx, the anterior stitch was adjusted and set at the amount of tension that gave the highest sound pressure level for subglottal pressures just above the phonation threshold pressure. The trachea was fitted over an aerodynamic nozzle that was designed to minimize turbulence and produce flow with a consistent velocity profile. The airflow entering the nozzle was controlled and measured using a coriolis flow meter (CMF025, Micro Motion; Boulder, CO), a pressure regulator (Model 700, ControlAir Inc, Amherst NH), and a mass flow controller (MPC 251, Parker; Cleveland, OH). Static pressure measurements were taken at the nozzle using a pressure transducer (PFG, Honeywell; Golden Valley, MN). In order to seed the flow, an atomizer was used (model 9306, TSI; Shoreview, MN) using DEHS oil (Bis[2-ethylhexyl] sebacate; Alfa Aesar, Ward Hill, MA). A schematic of the set-up is shown in Figure 5.

The PIV images were collected by illuminating the flow using a high repetition rate, dual cavity, Nd:YLF laser system (LDY304, Litron; Agawam, MA) synchronized with a high speed video camera (FASTCAM SA5, Photron; San Diego, CA). The camera lens was fitted with a 527nm band-pass filter to avoid reflections of the laser from the tissue. An area of 11.4×8.6 mm in the physical space was captured for each image, corresponding to a pixel resolution of 922×698 , respectively. Each image pair was taken at a time interval of $2.5 \mu\text{sec}$. Post-processing of the PIV data was done using DAVIS 8.0 software

(LaVision Inc, Goettingen, Germany) with a multipass decreasing window size (64×64 to 32×32) and adaptive interrogation window with 75% overlap.

The laser was focused and spread to produce a light sheet of 1-mm thickness in a mid-coronal plane halfway between the vocal process and the anterior commissure. It was placed such that the light sheet extended into the subglottis. The laser also reflected off the medial aspects of the folds, allowing for visualization of this tissue. The presence of the seeding particles allowed for clear differentiation between flow and the medial aspects of the fold. The mid-coronal plane was chosen because tissue displacements and the magnitudes of the velocities are usually highest in this section.

Flow measurements were taken by placing the PIV camera above the vocal folds in an oblique angle that is sufficient to visualize the intraglottal flow. For the canines used in this experiment, the vertical height of the folds was approximately 2 mm to 3 mm. The camera was tilted at an angle of 40° , which was sufficient to observe the entire flow from the inferior to superior aspect of the glottis. The oblique viewing angle caused a limited depth to the field of view, which was solved by attaching a Scheimpflug optical adaptor to the lens of the camera. The Scheimpflug adaptor brings the image into focus by tilting the image plane with respect to the orientation of the camera lens and light sheet. The use of this adaptor also introduces a strong perspective distortion; the factor of magnification is no longer constant across the complete field of view. The distortion is accounted for by applying polynomial mapping functions (3rd order) to the PIV. This technique is further described in Prasad et al.³¹

A downstream microphone ($1/2$ -inch free field microphone; Brüel & Kjær, 4950, Norcross, GA) was placed 5 cm to the side of the glottal exit in such a way that it did not interfere with laryngeal airflow. An electroglottograph (EGG) (KayPentax, Montvale, NJ) was used, and the electrodes were placed on both sides at the superior lateral aspect of the paraglottic space.

A high-speed video camera (Fastcam SA4, Photron; San Diego, CA) was placed approximately 1 meter above the glottal exit in order to visualize vocal fold vibration. The data from the microphone, pressure transducer, and EGG was digitized and recorded using a National Instruments (Austin, TX) PXI system. The timing and recording rates of all these systems were synchronized using a timing and synchronization module (National Instruments). All the systems shared a common trigger to start the acquisition of the data.

For all larynges, the phonation threshold pressure (PTP) and the phonation instability pressure (PIP) was determined using the method of Zhang et al.³² For each larynx, phonation trials were done at low, medium, and high subglottal pressures. The low and high pressures were set at approximately 2 centimeters (cm)H₂O above PTP and 2 cmH₂O below PIP, respectively. The middle subglottal pressure was set between the two. When the airflow was turned on, it took a few seconds for the phonation frequency to stabilize, which is why data collection started several seconds after the onset of phonation. Each phonation trial was approximately 1 second, allowing for collection of approximately 2,000 velocity fields.

The location of the medial aspect of the folds was determined from the PIV images in the coronal section. After all images were collected, they were sorted by phase and the images during the closing phase were selected. Using the method described by de Kat and van Oudheusden,³³ the measured velocities were then used to computationally determine the pressures from the Poisson equation, which is a simplified version of the generalized Navier-Stokes equations for fluid flow.

In order to use the Poisson equation, three assumptions are made: The first is that the flow in the midcoronal plane is two dimensional, or that there is no flow in the anterior-posterior direction. Khosla et al.³⁰ showed that in the mid-membranous location, the flow is two dimensional at the glottal exit and that the anterior-posterior flow starts at least 3 mm above the superior edge of the folds. The second is that the speed of the airflow in the inferior-superior direction is much greater than the speed of the folds in the medial-lateral direction. The magnitude of the former component is at least 40 times greater than the latter quantity in the experiments described in this article. The third is known as the "pseudo-steady hypothesis," which proposes that the dynamic vocal fold vibration can be modeled as a series of static vocal-fold coronal cross sections. As described previously, this coronal cross section is convergent during early to mid-opening, approximately straight at maximum opening, and then divergent during closing. Experimental and theoretical studies show that the pseudo-steady hypothesis is reasonable when the velocity of the airflow is not rapidly accelerating during the beginning of opening or rapidly decelerating during the end of closing.³⁴ Using this criterion, we show when the pseudo-steady hypothesis was reasonable in the next section. The combined validity of all three assumptions can be best evaluated by comparing these derived pressures with the actual intraglottal measurements in an excised hemilarynx.²⁶

RESULTS

In Figures 6 and 7, velocity fields and the medial shape of the folds are shown for larynx 1 at selected times during vocal fold closing. The left side of the figure represents the right fold and vice versa. These images were taken in the midcoronal plane. In the case of larynx 1, the low, mid-, and high subglottal pressures were 10 cmH₂O, 19.0 cmH₂O, and 25.5 cmH₂O, respectively.

An associated phase is given for each image, indicating the time in the vibration cycle that the velocity field was taken. The phases are measured in degrees such that 0 degrees is equivalent to 360 degrees and both occur when the superior edge of the folds start to come apart. This phase of the vibration cycle is defined as the beginning of opening and is determined by the high speed videography. The beginning of closing is defined as the phase when the inferior edge of the folds start to come together; the phase of both these events are determined from the high speed videography. As the subglottal pressure increased, the folds started to close earlier in the vibration cycle. Closing started at approximately 160 degrees for low pressure and at about 110 degrees for mid- and high pressures.

In Figures 6 and 7, the white lines represent the streamlines, which are lines connecting the velocity vectors at several points. The arrows mark the directions of the streamlines. When the streamlines are closer together, there is an increase in velocity and a decrease in pressure. For the low pressure in larynx 1, no flow separation was seen between the folds, and the folds did not have a divergent shape at any point during vocal fold closing. There were vortices above the folds, but the mechanism was not due to flow separation (see Khosla

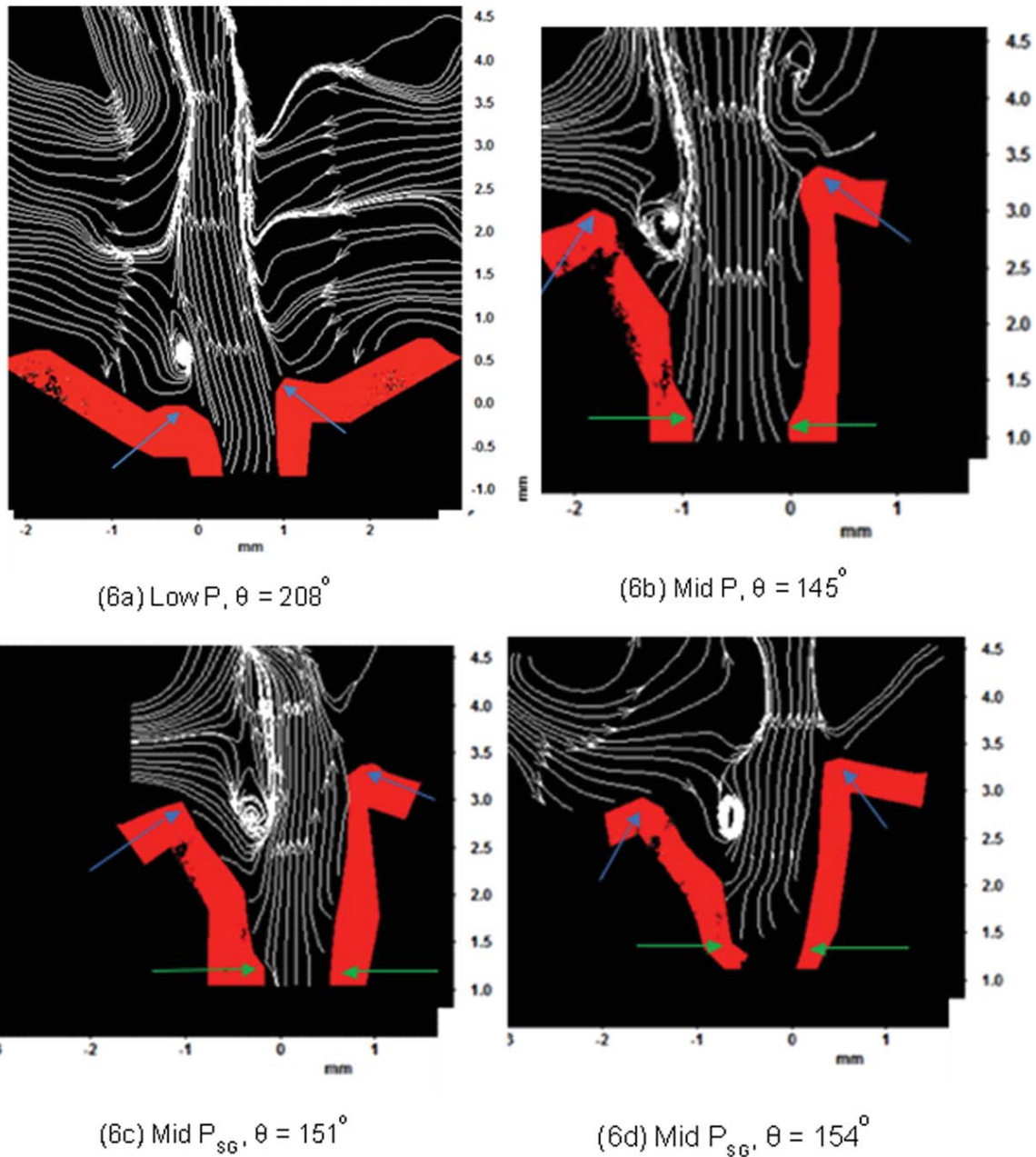
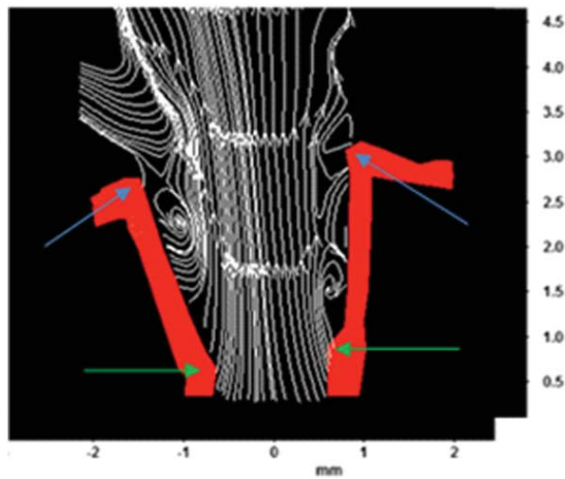


Fig. 6. Streamlines of the velocity fields (white lines) and the medial surface of the folds (most medial aspect of the red walls) for low and midsubglottal pressures at different phases during closing. The closer the streamlines, the faster the velocity. The highest velocities are seen in or around the vortices. The approximate location of the superior medial edge of the fold (blue arrows) and the inferior medial edge (green arrows) are shown. P_{SG} = subglottal pressure; θ = phase (see text for further description).

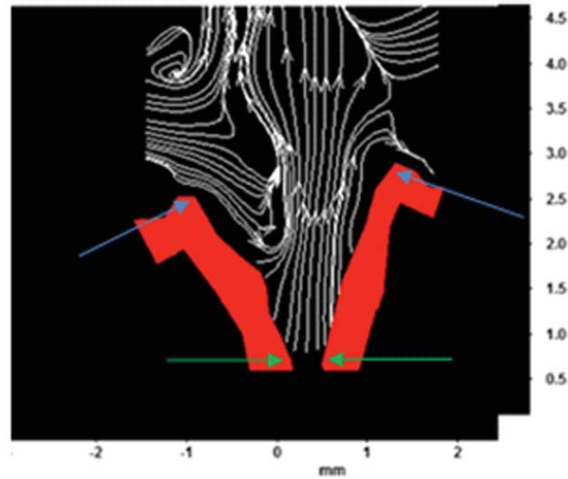
et al.²⁹ for an explanation of other mechanisms involved in producing vortices above the glottal exit). There was some mild curvature of the streamlines, which is predominantly due to the fact that the supraglottal jet tended to skew to one side. The skewing of the jet above the folds may be accentuated because there is no vocal tract in these experiments.

For the midsubglottal pressure in larynx 1, no flow separation was seen during approximately the first 35 degrees of closing and the velocities were predominantly unidirectional. At 145 degrees, there was a flow separa-

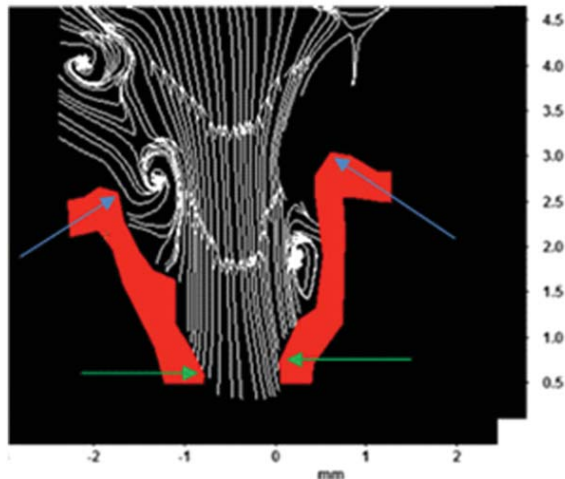
tion vortex adjacent to approximately the superior one-third of the right fold (left side of the image). The magnitudes of the associated negative pressures were greater at 151 degrees and even higher at 154 degrees. It can be seen that air from above the right fold entered into the glottis and became part of the vortical flow. This is because the vortex “sucks” in the surrounding flow, a process known in fluid mechanics as entrainment. This will be referred to as “air entrainment” to differentiate it from the term “entrainment” that is sometimes used to describe vocal fold vibration.



(7a) High P_{SG} , $\theta = 122^\circ$



(7c) High P_{SG} , $\theta = 140^\circ$



(7b) High P_{SG} , $\theta = 127^\circ$

Fig. 7. Streamlines of the velocity fields (white lines) and the medial surface of the folds (most medial aspect of the red walls) for high subglottal pressures at different phases during closing. (See text and figure 6 for further description.)

For the high subglottal pressure, no FSV were seen for approximately the first 10 degrees of closing. However, as is shown in Figure 7a, FSV on both sides were seen at 122 degrees. At 140 degrees, there was still rotational motion in the glottis on the right side, as well as air entrainment.

For the six other larynges, similar velocity fields were seen. The FSV were not seen at low pressures when the glottis was not divergent. In some cases, small vortices were present when the glottis had a small amount of divergence. The vortices were strong and usually on one side for the midpressures, and were very strong and on both sides for the high pressure. For each larynx, there were negative gage pressures only in the superior half of the larynx, and only when the FSV were produced.

The amount of negative pressure varied with the phase of the closing cycle and with the vertical location

in the glottis, depending on the location and strength of the rotational motion. In all larynges, flow separation started at or superior to the point halfway between the inferior and superior edges of the fold. The negative gage pressure with the highest absolute value, which we will define as the highest absolute negative pressure (HANP), was always found in the superior half of the glottis and occurred in the latter half of closing. Figure 8 shows the HANP as a function of phase during the closing for larynx 1 at mid- and high subglottal pressures. Since there were no negative intraglottal pressures for the low subglottal pressure, this case is not shown. It is observed that for the higher subglottal pressure, the HANP was larger and the duration was shorter; this trend was observed in all larynges. In general, HANP is associated with the strength of rotational motion in the FSV, which depends on a number of factors—including the size of the vortex and the speed of

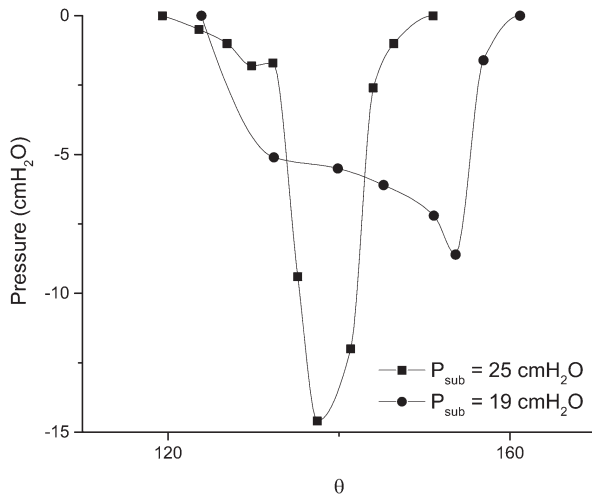


Fig. 8. Negative pressure (in cmH₂O) as a function of phase (θ).

flow in the vortex. In this article, a stronger FSV strictly means that there is stronger rotational motion; we do not quantify the specific factors accounting for this increase in FSV.

Figure 9 shows the relationships between the subglottal pressure and the HANP among all seven larynges. Each individual larynx has a correlation coefficient ranging from 0.96 to 0.99. The overall correlation coefficient is 0.965 (or slope \pm SE = 0.84 ± 0.08 , $P < 0.0001$) after combining all larynges using a mixed effect model to account for both within and between subject variations.³⁵

DISCUSSION

As discussed in the introduction, the absence of experimental measurements in the past resulted in the need to make one of the three intraglottal velocity field assumptions. Assumption 1 states that flow does not separate in the glottis during closing, and Bernoulli's law can be used along the entire vertical height of the glottis. Assumption 2 states that flow separates in the glottis and that intraglottal pressure downstream of the point of separation is zero gage pressure, which is defined as the pressure relative to atmospheric pressure. This assumption allows for the fact that FSV exist, but it states that the velocity fields of the FSV are negligible. Assumption 3 states that intraglottal FSV exist and that they produce negative pressures significantly below atmospheric pressure.

In all seven larynges, little to no intraglottal flow separation was seen at the low pressure. When small FSV were observed, the glottis was mildly divergent. The low subglottal pressure was set at 2 cm H₂O above the PTP. Use of Bernoulli's Law along the entire vertical height of the glottis (assumption 1) is accurate when there is no flow separation. However, flow separation was observed at mid- and high pressures. At the mid-pressure, the vortices formed on one side, as opposed to bilateral vortices seen at the higher pressure. The mid- and high subglottal pressures are associated with more

significant negative pressures relative to what has been previously predicted in most analytical and computational models^{3,11-13,15}; these models predict negative gage pressures of 0 to -2.0 cm H₂O in the superior aspect of the glottis. These predictions are consistent with the maximum negative pressures that were calculated when the subglottal pressure is low and FSV are small or nonexistent. However, when the FSV are present, the associated magnitudes of the negative pressures are significantly higher than the predicted values of 0 to -2.0 cm H₂O. Although the findings at mid- and high subglottal pressure demonstrate some disagreement with values predicted by theoretical models, our results are in accordance with data from Alipour and Scherer's study that experimentally measured intraglottal pressures in excised hemilarynges.²⁶

Despite the fact that this is the first laryngeal biomechanics study to report that intraglottal vortices produce negative pressure, similar effects of vortices are well known in other fields. Muijres et al. showed that slow flying bats produce vortices above their wings. These vortices produce negative, or suction, pressures, thereby generating lift.³⁶ CFD studies also show that coherent vortices provide additional mechanisms for lift in a hovering hawkmoth.³⁷ Experiments focusing on the fluid mechanics of heart valves revealed the existence of flow separation vortices, which are found to produce negative pressures that contribute to mitral valve closing.³⁸ Naguib et al.³⁹ experimentally studied the pressures that vortices induce on an adjacent wall and found significant negative pressures on that wall. In all these experiments, the negative pressure will decrease (have a higher absolute value) as the strength and size of the vortices increase.

The HANP reported may underestimate the effects of the vortices. The vortex produces pressure effects beyond its periphery. Thus, the pressures in the main jet or even on the opposite vocal fold may significantly change due to the vortex. For example, in a computational model using the appropriate methodology to simulate the vortices, Mihaescu et al.¹⁷ show that the

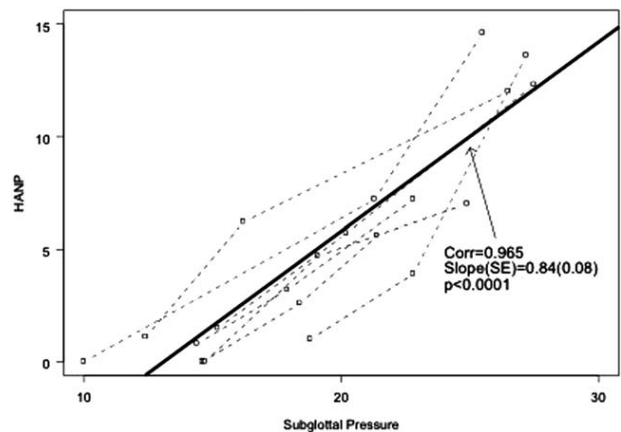


Fig. 9. Highest amplitude negative pressure (in cmH₂O) as a function of subglottal pressure. The dotted lines are the results for each larynx and the solid line is an average.

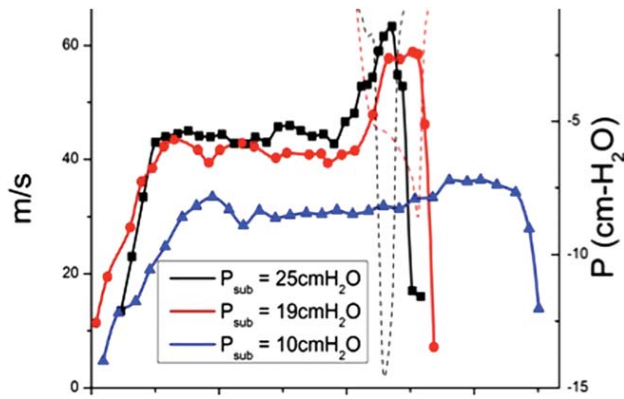


Fig. 10. Centerline velocity in meters per second (solid lines) for a low (10 cmH₂O), mid- (19 cmH₂O), and high (25 cmH₂O) subglottal pressures. The vertical axis for the velocity is on the left and for negative pressure (in centimeters of water) on the right. The negative pressures for the mid- (red dotted) and high subglottal pressures (black dotted) are shown.

vortices will produce negative pressures far beyond the periphery of the vortex. It was also indicated that negative pressures in the main jet are only about 10% lower in absolute value than at the center of the vortex. This low variation in horizontal pressures is commonly seen for jets in physical systems (such as the exit of an air-plane engine); the gradients are much larger in the main direction of the flow.¹⁸

The pressures reported in this article are computed from the measured velocity fields using Poisson's equation. The goal of these calculations is to give an order-of-magnitude estimate of the intraglottal pressures. Comparison of our negative intraglottal pressures with results from excised hemilarynx experiments by Alipour and Scherer²⁶ shows a similar range of values and waveform shapes for pressures in the mid-coronal plane of the superior glottis. For example, the pressure waveform at high subglottal pressures in Figure 8 are very similar to both the superior mid-membranous waveform in Alipour and Scherer's Figure 6 and to the waveform at the superior edge in Figure 9.²⁶ One limitation of the work performed by Alipour and Scherer is the lack of observation of vocal fold vibrations, which makes it difficult to quantitatively correlate the pressure measurements with the timing of the vibration cycle. However, the data produced in this study indicates the timing of the HANP in a variety of ways. One method is shown in Figure 10, which depicts both the centerline velocity during opening and closing and the pressure during closing as a function of phase. The pressures are shown as dotted lines and were previously shown in Figure 8. The centerline velocities are shown as solid lines and are defined as the maximum velocity in the inferior-superior direction at the glottal exit, which usually occurs at a point halfway between the folds and is measured from the velocity fields.

All velocity waveforms in Figure 10 have three phases: The first is rapid increase in velocity (high acceleration); the second is flat velocity with (at mid- and high subglottal pressures) or without (at low pressure) a

mild increase in velocity at the end (mild acceleration); and the third phase is a rapid velocity decrease (high deceleration). These three phases are described by Krane et al.³⁴ For both mid- and high subglottal pressures, the HANP occurs just before the end of closing. Krane et al.³⁴ also showed that the pseudo-steady hypothesis (discussed in the last section) is reasonable for the second phase only. Since the HANP occurs in the second phase, the pseudo-steady hypothesis is valid for calculating the negative pressures as the pressure values decrease but not as they increase during phase 3. The invalidity of the pseudo-steady hypothesis during phase 3 make the accuracy of the pressure calculations unknown, but we include them because the shape of the increase (Fig. 8 and Fig. 10) is in good agreement with the actual pressures measure in the hemilarynx.²⁶

The findings at mid- and high pressures show that FSV do exist and are associated with significant negative pressures. Thus, assumption 3 is valid for mid- and high pressures. Assumption 1 appears to be valid for low subglottal pressures. According to our data, there was no evidence to support assumption 2. In terms of physiological mechanisms, assumption 2 results in the prediction that the ERFs discussed in the introduction produced most of the forces responsible for vocal fold closing. This would suggest that the ERFs mostly determine the vocal fold closing speed (VFCS). Alternatively, we hypothesize that the negative pressures produced by the vortices result in an intraglottal negative pressure, which produce a "suction force" that also helps increase VFCS, as shown in Figure 4. Both the suction force and the ERFs are in the same direction, acting together to close the folds.

The effects on VFCS are important because an increase in VFCS will increase the maximum flow declination rate (MFDR), which is highly correlated with vocal intensity.⁴⁰ Stevens⁴ noted that the rapid reduction of flow rate is also important for generating acoustic energy over a broad frequency range and showed analytically that increasing the rate of flow shutoff will produce increased energy in the higher harmonics, a theory supported by findings in patients.^{41,42}

The negative pressures generated by the vortices only act during part of the closing phase, whereas the forces generated by tissue elasticity last during the entire closing cycle. However, the maximum VFCS may significantly increase if the forces produced by the negative pressures are strong enough, causing an increase in the MFDR. In order to determine the effect of the FSV relative to the effect of the ERFs on vocal-fold closing speed, tissue elasticity needs to be measured. These measurements will be taken in the future. Since increasing subglottal pressure increases both the FSV and the elastic recoil forces, the effect of the FSV on VFCS as compared to the elastic recoil forces will best be determined using a computational model where the two factors can be varied independently.

As discussed previously, the flow rate is equal to the area at the superior glottis multiplied by the velocity. Thus, the MFDR can increase by increasing the rate that the area decreases (which will happen if VFCS



Fig. 11. The formation of a boundary layer next to a wall (horizontal thick black line). The y-axis represents the relative distance away from the wall. The set of arrows on the left and right represent the velocity profiles at different distances from the wall; the length of the arrow is proportional to the magnitude of the velocity. The arrows indicate the flow is going in a left to right direction. The velocity is uniform on the left because those points are not adjacent to the wall. The velocity at the wall is zero, and the velocity profile on the right represents the boundary layer. (See text for further details.)

increases) and/or increasing the rate that velocity decreases. The latter is examined in Figure 10. It is seen that at low subglottal pressure, when there are no FSV, the centerline velocity waveform is relatively symmetrical. However, the waveform is very asymmetrical at mid- and high subglottal pressures because the velocity decreases much more rapidly than it increases. This asymmetry is known as skewing and is important acoustically because it results in increased MFDR and acoustic intensity. Clinically, skewing is important because it produces an increase in loudness without an increase in vocal fold trauma, whereas increasing the VFCS will increase the collision forces between the folds.

In current theoretical models, skewing of the velocity waveform is attributed solely to the inertance effects of the vocal tract; without a vocal tract, it is predicted that the velocity curve will be symmetrical.³ In our experiments, however, there is no vocal tract, and the velocity curve is only roughly symmetrical at low subglottal pressures when there are no FSV. Qualitatively, we have seen significant skewing of the velocity waveform in all seven larynges, but only when the FSV are present. Detailed analysis of these waveforms will be reported in future publications. Although these qualitative findings certainly do not definitively show that the FSV cause skewing, the effects of the FSV explain the phenomenon of skewing of the velocity waveform without a vocal tract, a phenomenon that previously has not been predicted by theoretical models. Thus, further exploration of the mechanisms of skewing will likely increase our knowledge of the relationship between vortices, vibration, and acoustics.

It is known that increasing subglottal pressure will increase MFDR and acoustic intensity.⁴¹ The current theory for this states that increasing subglottal pressure will increase the maximum lateral displacement of the vocal fold, which will increase the ERFs. This increase in ERFs will increase VFCS. However, the findings in this article suggest that increasing subglottal pressure also increases the strength of the FSV and the magnitude of the associated negative intraglottal pressures. As discussed previously, the FSV may increase MFDR by increasing both the VFCS and the skewing of the velocity waveform. Investigating these

underlying mechanisms of loud phonation is important for treating patients with voice disorders, especially those who have lost the ability to project their voice and cannot be understood in noisy conditions, as in a restaurant.

Given the above discussion, it is helpful to speculate how different laryngeal diseases or surgeries will affect the FSV. For this speculation, a basic knowledge of the mechanism of formation of the FSV is required. The velocity of fluid at the surface of any wall is zero, a phenomenon known as the “no-slip condition” that has been experimentally observed for all fluids. For a certain distance away from the wall, the velocity distribution of the adjacent fluid is changed due to the fluid’s viscosity. This distance is known as the boundary layer, and an example is shown in Figure 11. In this figure, the wall is shown as a black horizontal line. The vertical arrow represents the y axis, indicating the distance away from the plate. The flow is traveling from left to right, and the velocity profile to the left of the wall shows uniform velocities because there is no wall. However, as soon as the fluid goes past the wall, the velocity at the wall is zero. The viscous forces between layers of the fluid retard the velocity above the wall, which gives the velocity profile seen on the right. The length of the arrows represents the relative magnitude of the velocity. It is seen that the velocity increases as the distance away from the wall increases.

The velocity profile of the boundary layer will change if pressures are changing. For example, an APG (adverse pressure gradient, which means that the pressure is increasing) will cause the pressures to increase as the flow travels from left to right. This APG will push the fluid to the left and may cause fluid adjacent to the wall to move in an opposite direction. This phenomenon is known as reversal of flow^{18,19} and is shown in Figure 12. The reverse flow results in flow separation and the formation of vortices. Thus, in order to get flow separation vortices, there has to be a strong enough APG. The FSV will increase as the APG increases.

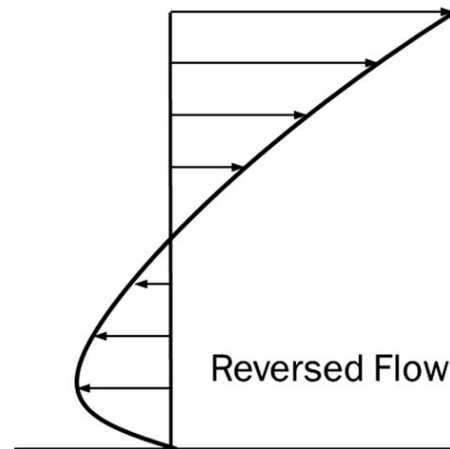


Fig. 12. The effect of an adverse pressure gradient (the pressure is increasing from left to right) on the boundary layer results in flow near the wall traveling in a reverse direction. This reversal of flow will produce rotational motion or fully formed vortices.

In fluid mechanics, it is known that the APG will increase and the FSV will be stronger as the amount of divergence, or the divergence angle, increases.¹⁸ It is reasonable to assume that the maximum divergence angle of the glottis will increase when the superior aspect of the fold is less stiff than the inferior aspect. This may explain the possible benefit of medializing the subglottis during a thyroplasty or injecting the subglottis during injection laryngoplasty. Although there is anecdotal evidence of the advantages of medializing the subglottis, there is neither reliable clinical evidence nor a reasonable theoretical explanation. However, it is possible that medializing the subglottis would lengthen the conus elasticus, which would likely increase the stiffness of the inferior edge of the fold. This hypothesis is consistent with experimental data that shows the inferior aspect of the fold to be stiffer than the superior aspect.⁹ Changing stiffness inferiorly relative to superiorly should increase the divergence angle. This hypothesis is undergoing current investigation in our lab. If the divergence angle is important, then scars, sulci, or small lesions at the inferior edge of the fold will be less acoustically important than if they are in the superior aspect of the fold.

Murugappan et al.⁴³ have shown that the FSV are markedly reduced or eliminated in the asymmetric vocal fold vibrations seen in unilateral vocal fold scarring, even in cases of observed periodic vocal-fold vibrations. If the FSV are important in normal phonation, the reduction or elimination of the FSV in voice disorders may be important in terms of understanding the underlying mechanisms. The effects of asymmetries in the mucosal wave on the FSV are currently being studied in our lab. We are also examining how surgical modifications can decrease or increase the FSV.

This study represents the first example of how intraglottal velocity fields and the geometry of the medial surface of both folds can be simultaneously measured in the excised larynx and how the findings can be used to yield interesting hypotheses. Although these hypotheses raise many questions that cannot be answered at this time, the experimental methodology developed in this project provides potential opportunities for future analysis via further experimentation and refined theoretical modeling.

CONCLUSION

Intraglottal velocity fields and glottal geometry were measured during the closing phase of vibration in a 1-mm thick coronal section. This section was taken at the mid-membranous location of the vocal folds. Flow separation vortices were seen at mid- to high subglottal pressures but were either minimal or absent at low subglottal pressures. When the FSV did exist, they produced negative pressures in approximately the superior half of the glottis. These negative pressures had a higher magnitude compared to the negative pressures found in a similar location, when the FSV did not exist. There was also skewing of the velocity waveform at mid- to higher subglottal pressures. This skewing was due to

the effects of the FSV, and the skewing should cause an increase in the MFDR and acoustic intensity. The combined data suggest that the FSV are not necessary for vocal fold vibration at low subglottal pressures but are important for increasing acoustic intensity and energy in the higher harmonics at mid- and high subglottal pressures.

ACKNOWLEDGEMENT

The authors would like to thank Gerald Berke MD, Randal Paniello MD, and Ron Scherer PhD for their help on this project.

BIBLIOGRAPHY

- Bertram CD. Flow-induced oscillations of collapsed tubes and airway structures. *Respir Physiol Neurobiol* 2008;163:256–265.
- Fant G. Preliminaries to analysis of the human voice source. *STL-QPRS* 1983;4:1–27.
- Titze IR. The physics of small amplitude oscillation of the vocal folds. *J Acoust Soc Am* 1988; 83:1536–1552.
- Stevens KN. *Acoustic Phonetics*. Cambridge, MA: MIT Press; 2000:75–126.
- Fant G. *Acoustic theory of speech production*. The Hague, Netherlands: Mouton; 1960.
- Van den Berg JW. Myoelastic-aerodynamic theory of voice production. *J Speech Hear Res* 1958;1:227–244.
- Hirano M. Morphological structure of the vocal cord as a vibrator and its variations. *Folia Phoniatr* 1974;26: 89–94.
- Berry DA, Montquin DW, Tayama N. High-speed digital imaging of the medial surface of the vocal folds. *J Acoust Soc Am* 2001;110: 2539–2547.
- Chhetri D, Zhang Z, Neubauer J. Measurement of Young's modulus of vocal folds by indentation. *J Voice* 2011;25:1–7.
- Goodyer EN, Muller F, Bramer B, Chauhan D, Hess M. In vivo measurement of the elastic properties of the human vocal fold. *Eur Arch Otorhinolaryngol* 2006;263:445–462.
- Ishizaka K, Flanagan JL. Synthesis of voiced sounds from a two-mass model of the vocal cords. *The Bell System Technical Journal* 1972;51: 1233–1267.
- Story B, Titze I. Voice simulation with a body-cover model of the vocal folds. *J Acoust Soc Am* 1995;97:1249–1260.
- Gunter HE. A mechanical model of vocal fold collision with high spatial and temporal resolution. *J Acoust Soc Am* 2003;113:994–1000.
- Dowell EH, Hall KC. Modeling of fluid-structure interaction. *Annual Review of Fluid Mechanics* 2001;33:445–490.
- Decker GZ, Thomson SL. Computational simulations of vocal fold vibration: Bernoulli versus Navier Stokes. *J Voice* 2007;21:273–284.
- Zhao W, Zhang C, Frankel SH, Mongeau L. Computational aeroacoustics of phonation, part 1: computational methods and sound generation mechanisms. *J Acoust Soc Am* 2012;112:2134–2146.
- Mihaescu M, Khosla SM, Murugappan M, Gutmark E. Unsteady laryngeal airflow simulations of the intra-glottal vortical structures. *J Acoust Soc Am* 2010;127:435–444.
- White, FM. *Fluid mechanics*. Boston, MA: McGraw-Hill; 1999: 59–214.
- Wu JZ, Ma HY, Zhou JZ. *Vorticity and vortex dynamics*. New York, NY: Springer; 2006: 201–382.
- Pelorsen X, Hirschberg A, Van Hassel RR, Wijnands APJ. Theoretical and experimental study of quasisteady-flow separation within the glottis during phonation. Application to a modified two-mass model. *J Acoust Soc Am* 1994;96:3416–3431.
- Hirschberg A. Some fluid dynamic aspects of speech. *Bull Comm* 1992; (part 2):1–30.
- Shinwari D, Scherer RC, Afjei A, Dewitt K. Flow visualization in a model of the glottis with a symmetric and oblique angle. *J Acoust Soc Am* 2003;113:487–497.
- Erath BD, Plesniak MW. An investigation of bimodal jet trajectory in flow through scaled models of the human vocal tract. *Experiments in Fluids* 2006;40:683–696.
- Pickup B, Thomson SL. Flow-induced vibratory response of idealized versus magnetic resonance imaging-based synthetic vocal fold mode. *J Acoust Soc Am* 2010;128:EL124–129. doi: 10.1121/1.3455876.
- Mihaescu M, Murugappan S, Kalra M, Khosla S, Gutmark E. Large Eddy Simulation and Reynolds-Averaged Navier-Stokes modeling of flow in a realistic pharyngeal airway model: an investigation of obstructive sleep apnea. *J Biomech* 2008;41:2279–2288.
- Alipour F, Scherer RC. Dynamic glottal pressures in an excised hemilarynx model. *J Voice* 2000;14:443–454.
- Berke GS, Moore DM, Monkewitz DA, Hanson DR, Gerratt BR. A Preliminary study of particle velocity during phonation in an in vivo canine model. *J Voice* 1989;3:306–313.

28. Bielamowicz S, Berke GS, Kreiman J, Gerratt B. Exit jet particle velocity in the in vivo canine laryngeal model with variable nerve stimulation. *J Voice* 1999;13:153–60.
29. Khosla S, Murugappan S, Gutmark E, Scherer RC. Vortical flow field during phonation in an excised canine larynx model. *Ann Otol Rhinol Laryngol* 2007;116:217–228.
30. Khosla S, Murugappan S, Lakhamraju, R, Gutmark E. Using particle image velocimetry to measure anterior-posterior velocity gradients in the excised canine larynx model. *Ann Otol Rhinol Laryngol* 2008;117:134–144.
31. Prasad AK, Jensen K. Scheimpflug stereocamera for particle image velocimetry in liquid flows. *Appl Opt* 1995;34:7092–7099.
32. Zhang Y, Reynders W, Jiang JJ, Tabeya I. Determination of phonation instability pressure and phonation pressure range in excised larynges. *J Speech Lang Hear Res* 2007;50:611–620.
33. de Kat R, van Oudheusden BW. Instantaneous planar pressure determination from PIV in turbulent flow. *Exp Fluids* 2012;52:1089–1106.
34. Krane MH, Barry M, Wei T. Dynamics of temporal variations in phonatory flow. *J Acoust Soc Am* 2010;128:372–383.
35. Roy A. Estimating correlation coefficient between two variables with repeated observations using mixed effects model. *Biom J* 2006;2:286–301.
36. Muijres FT, Johansson LC, Barfield R, Wolf M, Spedding GR, Hedenstrom A. Leading-edge vortex improves lift in slow-flying bats. *Science* 2008;319:1250–1253.
37. Liu H, Ellington CP, Kawach K, Berg CVD, Willmott A. A computational fluid dynamic study of hawkmoth hovering. *J Exp Biol* 1998;201:461–477.
38. Yoganathan AP, He Z, and Casey Jones S. Fluid mechanics of heart valves. *Annu Rev Biomed Eng* 2004;6:331–362.
39. Naguib AM, Koochesfahani MM. On wall-pressure sources associated with the unsteady separation in a vortex-ring wall interaction. *Phys Fluids* 2004;16:2613–2622.
40. Titze IR, Sundberg J. Acoustic intensity. Vocal intensity in speakers and singers. *J Acoust Soc Am* 1992;91:2936–2946.
41. Gauffin J, Sundberg J. Spectral correlates of glottal voice waveform characteristics. *J Speech Hearing Res* 1989;32:556–565.
42. Klatt DH, Klatt LC. Analysis, synthesis, and perception of voice quality variations among female and male talkers. *J Acoust Soc Am* 1990;87:820–857.
43. Murugappan S, Khosla S, Casper K, Oren L, Gutmark E. Flow fields and acoustics in a unilateral scarred vocal fold model. *Ann Otol Rhinol Laryngol* 2009;118:44–50.